A meshfree particle method with stress points and its applications at the nanoscale

Shaoping Xiao* and Weixuan Yang

Department of Mechanical and Industrial Engineering,
Centre for Computer-Aided Design,
University of Iowa, Iowa City, IA, USA
E-mail: shaoping-xiao@uiowa.edu
E-mail: weixuan-yang@uiowa.edu
*Corresponding author

Abstract: In this paper, a meshfree particle method with the stress point integration scheme is studied. It has been shown that this meshfree particle method with Lagrangian kernel can provide a stable method. A finite element mapping technique is introduced to insert stress points and to calculate volumes associated with particles/stress points so that the triangulation and the Voronoi diagram can be avoided. This meshfree particle method can be used for nanoscale simulations via the implementation of the Cauchy-Born rule. It can also be coupled with molecular dynamics based on the bridging domain coupling technique.

Keywords: meshfree particle method; Lagrangian kernel; stress points; stability; nanoscale.

Reference to this paper should be made as follows: Xiao, S. and Yang, W. (2006) 'A meshfree particle method with stress points and its applications at the nanoscale', *Int. J. Computational Science and Engineering*, Vol. 2, Nos. 3/4, pp.213–220.

Biographical notes: Shaoping Xiao received his PhD in Mechanical Engineering from Northwestern University in 2002. Currently, he is an Assistant Professor in the Department of Mechanical and Industrial Engineering, University of Iowa, Iowa City, IA, USA. He is also a Research Engineer affiliated with the Centre for Computer-Aided Design (CCAD) at the University of Iowa. His current research interests include computational nanotechnology, nanotube technology and computational solid mechanics.

Weixuan Yang is a Graduate Student in the Department of Mechanical and Industrial Engineering, University of Iowa, Iowa City, IA, USA. He is pursuing PhD in Mechanical Engineering under the supervision of Dr. Xiao. His current research focuses on nanoscale continuum modelling and simulation.

1 Introduction

There are two types of meshfree particle methods: field approximation based methods such as Element-Free Galerkin (EFG) methods (Belytschko et al., 1994) and kernel approximation based methods, such as Reproduced Kernel Particle Methods (RKPM) (Liu et al., 1996) and Smoothed Particle Hydrodynamics (SPH) (Randles and Libersky, 1996). The meshfree particle methods are advantageous to treat large deformation problems (Belytschko et al., 1997; Chen et al., 1998) as well as fracture problems (Krysl and Belytschko, 1999; Liu et al., 1999). There are two kernel functions used in the kernel based meshfree particle methods: the Lagrangian kernel, which is a function of the material coordinates and the Eulerian kernel, which is a function of the spatial coordinates. Belytschko and Xiao (2002) found that the kernel based meshfree particle methods had two instability properties: an instability due to rank deficiency and a tensile instability. Nodal integration scheme (Beissel and Belytschko, 1996) is usually used in kernel approximation based meshfree particle methods, but it results in the instability due to rank deficiency. As well, the tensile instability takes place due to the usage of Eulerian kernels. It has been shown that the additional quadrature points, that is, stress points, can eliminate the above instabilities if using Lagrangian kernels (Belytschko and Xiao, 2002; Rabczuk et al., 2004). In general, the triangulation and the Voronoi diagram are needed to accomplish the insertion of stress points and the calculation of volumes associated with particles/stress points for the stress point integration scheme. Such procedures will be complicated when irregular particle arrangement is considered as well three-dimensional problems. Alternatively, a finite element mapping technique will be introduced in this paper to insert stress points and to calculate volumes associated with particles/stress points.

Numerical simulation has become a powerful tool and has made a significant contribution to nano science and technology. Continuum methods, typically finite element methods, can be used to model and simulate large nano systems via the homogenisation technique, that is, the Cauchy-Born rule (Milstein, 1982). This continuum approach, known as one of hierarchical multiscale methods, is also called the quasicontinuum method (Tadmor et al. 1996). Rodney and Phillips (1999)

generated quasicontinuum simulations of dislocations lying in intersecting slip planes, and calculated the threshold stress required to break the dislocation junction. Shenoy et al. (1999) developed a finite-temperature quasicontinuum method. Chen et al. (2005) developed a Discontinuous Galerkin (DG) method, within the framework of the Heterogeneous Multiscale Method (HMM), to solve hyperbolic and parabolic multiscale problems.

Another multiscale modelling is called concurrent multiscale modelling, in which continuum methods are coupled with molecular methods. In a pioneering work, Abraham et al. (1998) developed the Macro-Atomistic-Ab initio-Dynamics (MAAD) methodology, in which a tight-binding quantum mechanical calculation is coupled with MD and in turn, coupled with a finite element continuum model. Recently, various concurrent multiscale techniques, particularly coupling methods between continuum and molecular models, have been developed. Park et al. (2005) developed a multiscale method in which the molecular displacements are decomposed into fine scale (molecular) and coarse scale (continuum). Belytschko and Xiao (2003) (Xiao and Belytschko, 2004) coupled molecular dynamics with continuum mechanics via a bridging domain. Fish and Chen (2004) proposed a concurrent multiscale approach based on multigrid principles with the intent of solving large molecular dynamics systems.

Since meshfree particle methods are more attractive for usage in a variety of situations (Belytschko et al., 1997; Chen et al., 1998; Krysl and Belytschko, 1999; Liu et al., 1999), including problems with moving boundaries, discontinuities and extremely large deformations, the incorporation of them with a homogenisation technique will benefit the multiscale methods at the nanoscale.

The outline of this paper is as follows. A meshfree particle method is introduced in Section 2. A finite element mapping technique for the insertion of particles/stress points and their volume calculation is proposed to avoid usage of the triangulation and the Voronoi diagram. Section 3 will describe the implementation of the Cauchy-Born rule into the meshfree particle method. A concurrent multiscale method, in which the meshfree particle method is coupled with molecular dynamics, is also proposed. Several examples are studied in Section 4 followed by the conclusions.

2 Meshfree particle method

2.1 Governing equations

The Galerkin weak form of the momentum conservation equation is

$$\int_{\Omega_0}\delta u_i\rho_0\ddot{u}_i d\Omega_0=\int_{\Omega_0}\delta u_i\rho_0 b_i d\Omega_0 -\int_{\Omega_0}\frac{\partial(\delta u_i)}{\partial X_j}P_{ji}d\Omega_0+\int_{\Gamma_0}\delta u_i\bar{t}_i d\Gamma_0 \tag{1}$$

where ρ_0 is the initial density, P is the first Piola-Kirchhoff stress tensor, $\mathbf{X}$ are the material (Lagrangian) coordinates, $\boldsymbol{b}$ is the body force per unit mass, δ_u is the test function, $\bar{\boldsymbol{t}}$ is the prescribed boundary traction and $\boldsymbol{u}$ is the displacement and the superposed dots denote material time derivatives.*

Equation (1) is written in the reference configuration, Ω_0, with the boundary, Γ_0. In meshfree particle methods, the field of displacements, $\boldsymbol{u}^h(\mathbf{X}, t)$, are approximated by

$$u^h(\mathbf{X},t)=\sum_I w_I(\mathbf{X})u_I(t) \tag{2}$$

where $w_I(\mathbf{X})$ are called Lagrangian kernels because they are functions of the material (Lagrangian) coordinates, $\mathbf{X}$. If the kernel functions are functions of the spatial (Eulerian) coordinates, $\mathbf{X}$, they are called Eulerian kernels. In this paper, we use Lagrangian kernels unless otherwise noted. The Lagrangian kernel functions are calculated from weight functions, $W(\mathbf{X})$ that is,

$$w_I(\mathbf{X})=w(\mathbf{X}-\mathbf{X}_I)=\frac{W(\mathbf{X}-\mathbf{X}_I)}{\sum_K W(\mathbf{X}-\mathbf{X}_K)} \tag{3}$$

In our analysis, a quartic spline weight function is used:

$$W(R)=\begin{cases}1-6\left(\frac{R}{R_0}\right)^2+8\left(\frac{R}{R_0}\right)^3-3\left(\frac{R}{R_0}\right)^4 & R\le R_0\\ 0 & R\le R_0\end{cases} \tag{4}$$

where $R=\mathbf{X}-\mathbf{X}_J$ and R_0 is the support radius.

It is obvious that the kernel functions reproduce the constant functions that is, $\sum_I w_I(\mathrm{X})=1$, but not the linear functions. In other words, one can find that $\sum_I w_{I,i}(\mathbf{X})X_{Ij}\neq\delta_{ij}$. A correction, developed by Belytschko et al. (1998), is used to enable the derivatives of constant or linear functions to be reproduced exactly.

Substituting Equation (2) into the weak form of Equation (1), the following discrete equations of motion are derived:

$$m_I\ddot{u}_{iI}=F_{iI}^{\text{ext}}-F_{iI}^{\text{int}}, m_I=\rho_0 V_I^0 \tag{5}$$

where m_I represents the mass of the particle I, V_I^0 is the volume associated with this particle, F_{iI}^{ext} are the external nodal forces and F_{iI}^{int} are the internal nodal forces given by

$$F_{iI}^{int}=\int_{\Omega_0}\frac{\partial w_I(\mathbf{X})}{\partial X_j}P_{ij}d\Omega_0 \tag{6}$$

It should be noted here that Equation (5) can be rewritten as the discrete equations for static problems by setting accelerations zero.

2.2 Numerical integration

EFG method (Belytschko et al., 1994) needs a background mesh so that Gaussian quadratures can be used for numerical integration of Equation (6), but it is computationally intensive. Beissel and Belytschko (1996) proposed nodal integration to reduce the computer time and the internal forces are calculated via

$$f_{iI}^{\text{int}}=\sum_{J\in N_M}V_J^0\frac{\partial w_I(\mathbf{X}_J)}{\partial X_j}P_{ji}(\mathbf{X}_J) \tag{7}$$

However, it will result in one of the instabilities due to rank deficiency for some problems (Belytschko and Xiao, 2002). The stress point integration scheme (Dyka et al., 1997) was proposed to stabilise this instability. Stress points play the same role as additional quadrature points during numerical integration. Those additional quadrature points are called slave points/particles and the original particles are called master particles. The motion of stress points is completely determined by the motion of master particles through kinetics relations. In other words, the kinetic variables of stress points, such as displacements and velocities, are evaluated from the neighbouring master particles by the approximation Equation (2). Discrete equations, Equation (5), are only solved for motion of master particles.

According to the stress point integration scheme, the integration for internal forces is thereafter written as

$$f_{iI}^{\text{int}} = \sum_{J\in N_M} V_J^{0M} \frac{\partial w_I(\mathbf{X}_J^M)}{\partial X_j} P_{ji}(\mathbf{X}_J^M) + \sum_{J\in N_S} V_J^{0S} \frac{\partial w_I(\mathbf{X}_J^S)}{\partial X_j} P_{ji}(\mathbf{X}_J^S) \tag{8}$$

where '*M*' represents master particles, while '*S*' represents stress points. N_M and N_S are the sets of master particles and stress points, respectively, which contribute to the master particle at $\mathbf{X}_I^M$. The volumes V_J^{0M} and V_J^{0S} are the volumes associated with master particles and stress points. They are different from V_J^0 in Equation (5) and $\sum V_J^0 = \sum V_J^{0M} + \sum V_J^{0S}$. Those volumes are usually computed from a Voronoi diagram.

2.3 Stability analysis

In a linearised stability analysis (Belytschko and Xiao, 2002), we investigate the stability of the slab to a perturbation in the displacement. The perturbation can be expressed as $\mathbf{x} = \bar{\mathbf{x}} + \tilde{\mathbf{x}}$. $\tilde{\mathbf{x}}$ is a plane wave perturbation as

$$\tilde{\mathbf{x}} = \tilde{\boldsymbol{u}} = g e^{i\omega t + i\kappa n_0 X} \tag{9}$$

where, κ is wave number, ω is frequency and $\boldsymbol{g}$ is polarisation of the wave. Equation (9) can be substituted into governing equations or discrete equations to obtain the characteristic equations, which can be solved for frequencies.

An isotropic hyperelastic material (Belytschko et al., 2000) is considered here. Its potential is given by

$$\psi = \frac{1}{2}c_1 I_1 + \frac{1}{2}c_2 I_2 - \left[\frac{3}{2}c_1 I_3^{\frac{1}{3}} + \frac{3}{2}c_2 I_3^{\frac{2}{3}} - \frac{\lambda}{4}\left(\ln I_3\right)^2\right] \tag{10}$$

where I_1, I_2 and I_3 are the principal invariants of the right Cauchy-Green deformation tensor $\mathbf{C}$. The constitutive relationship can be derived via obtaining the second Piola-Kirchhoff stress tensor from the first derivatives of potential function with respect to the right Cauchy-Green deformation tensor. In this paper, the following materials are considered constants: C_1 = 0.1256MPa, C_2 = 0.01012MPa and λ = 10.12MPa. To simplify the analysis, we consider a diagonal deformation gradient $\boldsymbol{F}$ for the initial state of deformation, which is characterised by three stretches, λ_i (λ_3 is assumed to be 1 here). For a given deformation, the frequency of the plane wave perturbation can be obtained by solving the characteristic equations. If there exists ω such that $\text{Im}(\omega) < 0$, the simulated system will be unstable. Stable domains for the considered material are shown in Figure 1. The exact solution was obtained from the linearised stability analysis of the governing equations, that is, PDEs and it represents the material stability itself. From Figure 1, it can be seen that the Lagrangian kernel can exactly reproduce the material instability, but the Eulerian kernel severely distorts it.

Figure 1 Stable domains of the meshfree particle method with stress points (a) Lagrangian kernel and (b) Eulerian kernel

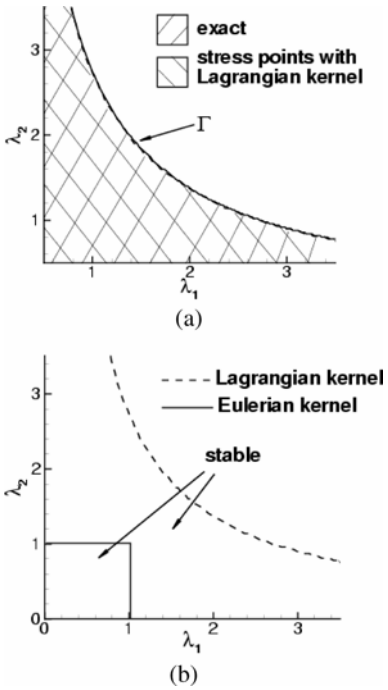

2.4 Insertion of stress points

In meshfree particle modelling of an object with arbitrary geometry, master particles are arranged irregularly. Triangulation is usually conducted to construct a triangular (or tetrahedral in 3D) mesh as shown in Figure 2(a). Master particles are vertices of those triangles. The stress points are then inserted at the centre of triangles (or tetrahedrons). Next, the Voronoi diagram is performed to generate Voronoi cells for both master particles and stress points, as shown in Figure 2(b). The volumes of these cells are calculated as V_J^{0M} and V_J^{0S} for the stress point integration scheme as in Equation (8). However, since the algorithms of triangulation and Voronoi diagram are complicated, especially for three-dimensional problems, they are not applicable for multiple dimensional problems with an arbitrary geometry. In this paper, we introduce a simple technique of finite element mapping to insert stress points and to calculate volumes associated with master particles and stress points.

Figure 2 Stress point insertion and volume calculation (a) Triangulation and (b) Voronoi cells

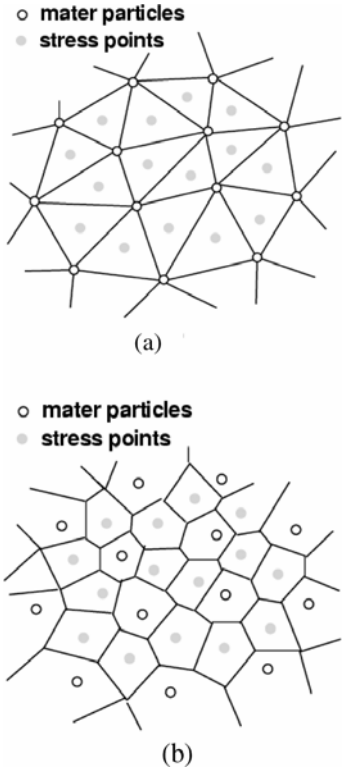

With current powerful finite element mesh generation software it is easy to construct triangular or tetrahedral meshes in the reference configuration for any given problem. The nodes can be taken as master particles in meshfree particle methods. In finite element methods, the reference configuration can be mapped from the parent configuration (Belytschko et al., 2000) via $\mathbf{X} = \mathbf{X}(\xi)$ where ξ represents coordinates in the parent configuration. If stress point I is at the centre of an equilateral triangle ABC in the parent configuration as shown in Figure 3, the co`ordinate of this stress point in the reference configuration can be obtained via the finite element approximation, which is

$$\mathbf{X}^S\left(\xi_I\right) = \sum_J N_J\left(\xi_I\right)\mathbf{X}_J^M, \quad J = A,B,C \tag{11}$$

where $N(\xi)$ are finite element interpolation functions evaluated in the parent configuration. In other words, stress points are also inserted at the centres of triangular meshes in the reference configuration.

Figure 3 The finite element mapping technique

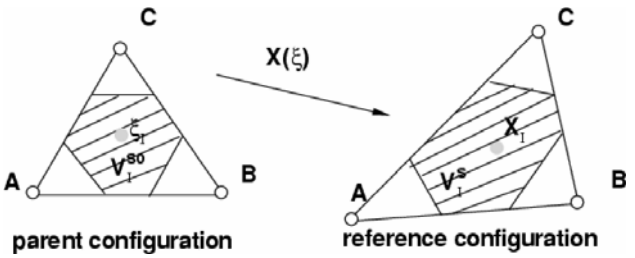

In the parent configuration, it is easy to calculate volume V_I^0 of the Voronoi cell, which is associated with stress point I. Through the finite element mapping technique, the volume associated with this stress point in the reference configuration is calculated by:

$$V_I^S = \det\left(\mathbf{F}\left(\xi_I\right)\right)V_I^{S0} \tag{12}$$

where $\mathbf{F}\left(\xi_I\right) = \left.\dfrac{\partial \mathbf{X}(\xi)}{\partial \xi}\right|_{\xi_I} = \left(\sum_J \dfrac{\partial N_J(\xi)}{\partial \xi}\mathbf{X}_J^M\right)\Bigg|_{\xi_I}$ is the gradient of the mapping function evaluated at stress point I in the parent configuration. A similar procedure can be performed to calculate volumes associated with master particles in the reference configuration.

3 Meshfree particle methods at the nanoscale

3.1 Implementation of the Cauchy-Born rule

With a homogenisation technique, such as the Cauchy-Born rule (Chen et al., 1998), it is possible to impose the continuum mechanics methods to perform simulations at the nanoscale because the intrinsic properties of material can be sought at the atomic level and embedded in the continuum. Such methods are also called the hierarchical multiscale methods. Finite element methods are always used in multiscale methods with the implementation of the Cauchy-Born rule. Since the meshfree particle methods are advantageous to treat large deformation problems as well as fracture problems, they will have potential to be used in nanoscale numerical modelling and simulation. The Cauchy-Born rule states the deformation is locally homogeneous, so it is assumed there is a constant gradient of deformation in each volume that is associated with a master particle or a stress point.

As Figure 4 shows, an undeformed lattice vector **A** in the reference configuration is mapped into **a** in the current configuration by the gradient of deformation **F** via **a = FA**. In the continuum model, the potential energy depends on the elongations and angle changes of the atomic bonds that underlie the volume of master particles or stress points. The total potential of the continuum model is defined by

$$W^C = \int_{\Omega_0} w_C\left(\mathbf{F}\right)d\Omega \tag{13}$$

where w_c is the potential energy per unit volume. Then, the first Piola-Kirchhoff stresses, ***P***, at master particles or stress points are computed as follows

$$\begin{aligned} \boldsymbol{P}\left(\mathrm{X}_I^M\right) &= \frac{\partial w_C\left(\mathbf{F}\left(\mathbf{X}_I^M\right)\right)}{\partial \mathrm{F}\left(\mathbf{X}_I^M\right)}, \\ \boldsymbol{P}\left(\mathbf{X}_I^S\right) &= \frac{\partial w_C\left(\mathbf{F}\left(\mathbf{X}_I^S\right)\right)}{\partial \mathbf{F}\left(\mathbf{X}_I^S\right)} \end{aligned} \tag{14}$$

where

$$\begin{aligned} \mathbf{F}\left(\mathbf{X}_I^M\right) &= \sum_J \frac{\partial w_J\left(\mathbf{X}_I^M\right)}{\partial \mathbf{X}}\boldsymbol{u}_J^M, \\ \mathrm{F}\left(\mathbf{X}_I^S\right) &= \sum_J \frac{\partial w_J\left(\mathbf{X}_I^S\right)}{\partial \mathbf{X}}\boldsymbol{u}_J^M \end{aligned} \tag{15}$$

Equation (14) serves as the constitutive equation for the meshfree particle method based on atomistic potentials via the Cauchy-Born rule. However, the Cauchy-Born rule has some difficulties for many important situations, such as in single-layer curved crystalline sheets. Therefore, an extension of the Cauchy-Born rule – the exponential Cauchy-Born rule developed by Arroyo and Belytschko (2002) – will be used for those simulations.

Figure 4 Cauchy-Born rule in meshfree particle methods

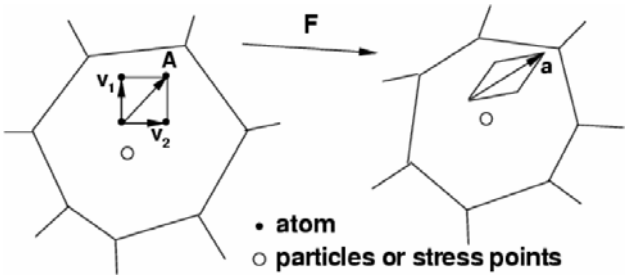

3.2 Coupling of the meshfree particle method with molecular dynamics

With the development of multiscale modelling at the nanoscale, Xiao and Belytschko (2004) proposed a bridging domain coupling method. In this paper, this technique is used to develop a concurrent multiscale model in which the meshfree particle method is coupled with molecular dynamics. In expressing the total Hamiltonian of the system, a scaling parameter β in the bridging domain, Ω_0^{int}, which is the overlapping domain between the molecular domain, Ω_0^M and the continuum domain, Ω_0^C, as shown in Figure 5, is employed. The Hamiltonian, H, for the complete domain is taken to be a linear combination of the molecular and continuum Hamiltonians, as shown in

$$\begin{aligned} H &= \beta H^M + (1-\beta) H^C \\ &= \sum_I \beta(\mathbf{X}_I)\frac{1}{2} m_I \dot{\boldsymbol{d}}_I \dot{\boldsymbol{d}}_I + \sum_I \beta(\mathbf{X}_I) W^M(\mathbf{X}_I) \\ &+ \sum_I \left(1-\beta(\mathbf{X}_I)\right)\frac{1}{2} M_I \dot{\boldsymbol{u}}_I \dot{\boldsymbol{u}}_I + \\ &\int_{\Omega_0} \left(1-\beta(\mathbf{X})\right) w_C\left(\mathbf{F}(\mathbf{X})\right) d\Omega \end{aligned} \tag{16}$$

where m_I and M_I are mass for atoms and master particles, respectively. W^M is the potential function in the molecular model. H^M and H^C are molecular and continuum Hamiltonians, respectively. $\boldsymbol{d}$ are atomic displacements.

The constraints in the bridging domain are

$$\boldsymbol{g}_I = \{\boldsymbol{g}_{iI}\} = \{u_i(\mathbf{X}_I) - \boldsymbol{d}_{iI}\} = \left\{\sum_J w_J(\mathbf{X}_I)\boldsymbol{u}_{iJ} - \boldsymbol{d}_{iI}\right\} = 0 \tag{17}$$

that is, the atomic displacements, $\boldsymbol{d}$, are required to conform to the continuum displacements, $\boldsymbol{u}$, at the positions of the atoms. The continuum displacement field can be obtained from the meshfree particle approximation as Equation (2). The constraints are applied to all components of the displacements. With the Lagrange multiplier method, the total Hamiltonian is written as

$$H_L = H + \lambda^T \mathbf{g} = H + \sum_I \lambda_I^T \mathbf{g}_I \tag{18}$$

where $\lambda_I = \{\lambda_{iI}\}$ is a vector of Lagrange multipliers. Note that the Lagrange multipliers are assigned to the discrete positions of atoms in the bridging domain.

Figure 5 A bridging coupling model for a molecular chain

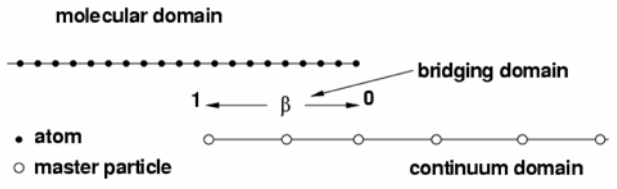

The discrete equations can be derived from Equation (18) via classical Hamiltonian mechanics. In equations of motion there exist constraint forces applied on the atoms/particles in the bridging domain besides external and internal forces. Xiao and Belytschko (2004) developed an explicit time integration algorithm. At first, so-called trial velocities are obtained by solving equations of motion independently in the continuum and molecular domains without the consideration of constraints. Then, constraints are applied to calculate the Lagrange multipliers. Finally, the constraint forces are considered to correct the velocities of atoms/particles in the bridging domain. The details can be found in Xiao and Belytschko (2004).

4 Examples

4.1 Taylor bar impact

A classical benchmark problem, the Taylor bar impact, is examined here. In this example, a cylindrical bar impacts a rigid, frictionless anvil with an initially high speed, 227 m/s. Von Mises J_2 flow theory (see Belytschko et al., 2000) with linear isotropic hardening is applied for the computation. The material data are: density ρ = 8930 kg/m^3, Young's modulus E = 117 GPa, Poisson's ratio μ = 0.35, plastic modulus E_P = 100 MPa and yield strength σ_Y = 400 MPa.

Table 1 Results of meshfree particle methods comparing with DYNA3D

Particles number	*Stress points number*	*Final radius (mm)*	*Final length (mm)*	*Maximum plastic strain*
520	1920	6.88	21.70	2.10
6171	30000	7.02	21.47	3.16
	DYNA3D	7.03	21.47	2.96

In this three-dimensional example, the tetrahedral arrangement of master particles is considered based on finite element mesh generation. Master particles are placed on the vertices of tetrahedrons. Based on the finite element approximation and mapping as described in Section 2.3, the positions of stress points in the reference configuration, as well as the volumes associated with master particles and stress points, can be obtained. Here, an equilateral

tetrahedron is considered as the parent element. Figure 6 shows deformed shapes and the equivalent plastic strain evolution of the middle section of the Taylor bar. The results shown in Table 1 are in good agreement with the ones from DYNA3D.

Figure 6 Effective plastic strain evolution in Taylor bar (a) t = 0.015 ms (b) t = 0.03 ms and (c) t = 0.06 ms

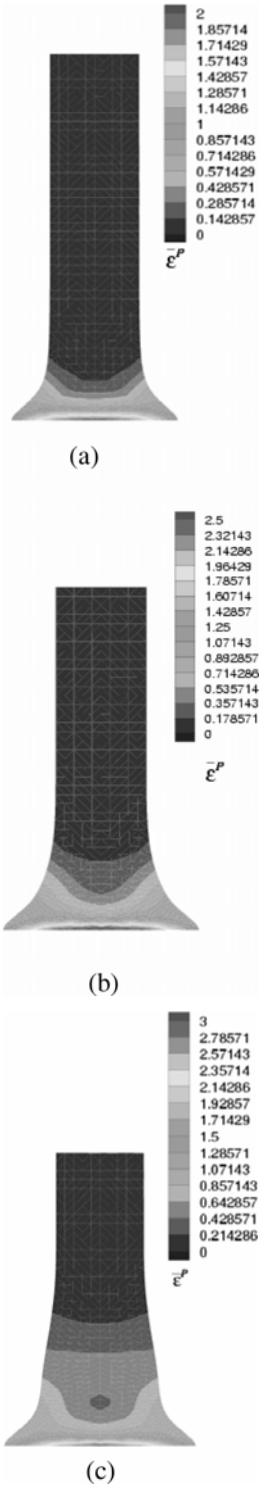

4.2 Wave propagation in a molecule chain

In this example, the wave propagation in a molecular chain, which contains 2001 atoms, is simulated. The LJ 6–12 potential function is used as the interatomic potential function between the nearest atoms, and it is

$$w_M = 4\varepsilon\left[(\sigma/r)^{12} - (\sigma/r)^{6}\right] \tag{19}$$

where the constants are chosen as: σ = 3.4e^{-10}m and ε = 1.65e^{-21}J. The mass of each atom is set to be 3.8×10^{-10} kg.

Figure 7 The initial wave in a molecule chain

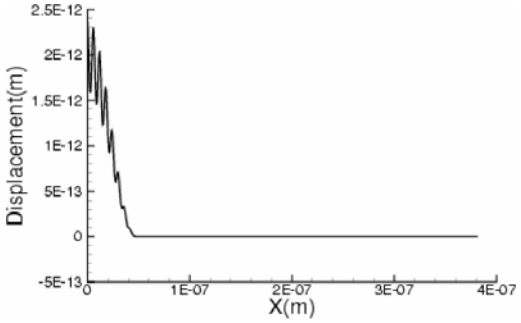

In the bridging domain coupling modelling of this molecule chain, there are 1001 atoms in the molecular domain and 100 master particles in the continuum domain. The initial wave is the combination of high frequency and low frequency waves as shown in Figure 7 in the molecular domain.

A handshake technique (Broughton et al., 1999) was developed for coupling a finite element method and molecular dynamics. In that method, the element size was graded down to the lattice spacing in the handshake region. This technique will result in a non-physical phenomenon as shown in Figure 8(a) at the interface between the continuum domain and the molecular domain if the artificial viscosity is not applied. We can see that high frequency waves are reflected while the low frequency wave passes the continuum domain. Such a phenomenon is also called spurious wave reflection. However, with the bridging domain coupling technique, the spurious wave reflection can be eliminated as shown in Figure 8(b).

Figure 8 Multiscale methods simulations (a) handshake method and (b) bridging domain coupling method

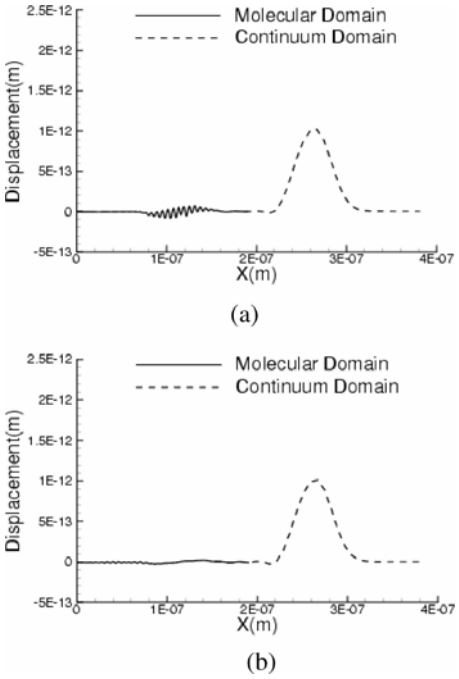

4.2 A nanoplate with a central crack

Since meshfree particle methods are beneficial in treating fracture problems, in this example the meshfree particle method with the implementation of the Cauchy-Born rule will be used to study the stress concentration of a nanoplate containing an initial central crack. The dimensions of the nanoplate are: a length of 270 nm and a width of 280 nm. The crack is initialised by taking a number of bonds out and the initial crack length is 135 nm. This nanoplate contains 86,915 atoms with the triangular/hexagonal molecular structure. The meshfree particle model contains 400 master particles and 722 stress points. The LJ (6–12) potential function in Equation (19) is used in this example with the following constants: σ = 1.833 nm and $\varepsilon = 8.25e^{-9}$J. A visibility criterion in the meshfree particle model is used to construct the kernel functions for the particles near the crack or around the crack tip.

In this example, the bottom of the nanoplate is fixed while prescribed displacements are applied on the top of the nanoplate. The constitutive relationship can be achieved through the Cauchy-Born rule, that is, Equation (14). For the purpose of comparison, molecular mechanics calculations are also performed. Computation time for molecular mechanics calculation is 2400 sec, which is dramatically reduced to 10 sec for meshfree particle simulation. Figure 9 shows that the evolution of potential obtained from the meshfree particle method is in accord with the evolution of potential from the molecular mechanics calculation. If more particles, for example, 900 particles, are employed, the comparison is more advantageous, as shown in Figure 9.

Figure 9 Comparison of potential between the meshfree particle method and molecular mechanics calculation

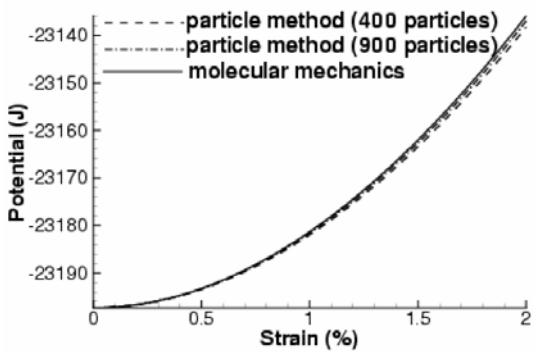

Figure 10 Convergence of the meshfree particle method

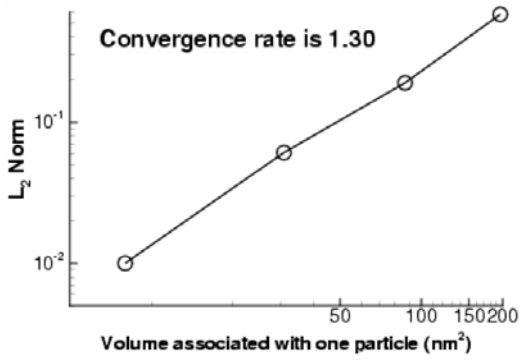

We study the convergence by using the l_2 error in displacement for the meshfree particle method as shown in Figure 10. The error in displacement is defined as

$$\text{Error} = \frac{\left\| \boldsymbol{u}^{MM} - \boldsymbol{u}^{PM} \right\|_2}{\left\| \boldsymbol{u}^{MM} \right\|_2} \tag{20}$$

where $\boldsymbol{u}^{MM}$ and $\boldsymbol{u}^{PM}$ are the atomic displacements from the molecular mechanics calculation and the meshfree particle method, respectively. Note here that one can calculate the atomic displacements from the particle displacements in the meshfree particle method based on the meshfree particle approximation, that is, Equation (2). The norm is defined as follows:

$$\left\| \boldsymbol{u} \right\|_2 = \left(\int_\Omega \left\| \boldsymbol{u} \right\|^2 \right)^{1/2} \tag{21}$$

As well, we investigate the stress concentration around the crack tip while the nanoplate is under the uniaxial strain of 2%. At the atomic level, the Cauchy stress is calculated as the following formula:

$$\sigma = \frac{1}{\Omega} \sum_i^N \left(\frac{1}{2} \sum_{j \neq i} r_{ij} \otimes f_{ij} \right) \tag{22}$$

where $r_{ij} = r_i - r_j$ is the spatial vector between atoms i and j, and $\otimes$ denotes the tensor product of two vectors. The interatomic force $\mathbf{f}_{ij}$ applied on atom i by atom j is:

$$\boldsymbol{f}_{ij} = -\frac{\partial \phi_{ij} r_{ij}}{\partial r_{ij} r_{ij}} \tag{23}$$

where Φ_{ij} is the interatomic potential between atoms i and j. The sign is adopted here for force, which is positive for repulsion and negative for attraction.

Figure 11 shows the comparison of the stress (σ_{yy}) contour between the molecular mechanics calculation and the meshfree particle simulation. It can be seen that the contours are in accord except the difference of stress concentration area at the crack tip. We think that such difference is due to coarse particle approximation at the crack tip, which can be improved by inserting more particles around that specific area.

5 Conclusions

The meshfree particle method with a Lagrangian kernel and the stress point integration scheme is introduced in this paper since this method has been proved to be a stable and efficient meshfree particle method. We impose finite element approximating and mapping techniques to perform insertion of stress points and volume calculation for master particles and stress points. As a result, the triangulation and the Voronoi diagram can be avoided since they create complications for engineers, especially in three-dimensional simulations. Furthermore, we implement the Cauchy-Born rule into the meshfree particle method for nanoscale modelling and simulation. Therefore, the meshfree particle method can be used to approach a large group of atoms. Such a hierarchical

multiscale method can provide good results when compared with molecular mechanics simulations. As well, the meshfree particle method can also be coupled with molecular dynamics in concurrent multiscale modelling.

Figure 11 Comparison of stress concentration (a) molecular mechanics and (b) meshfree particle method

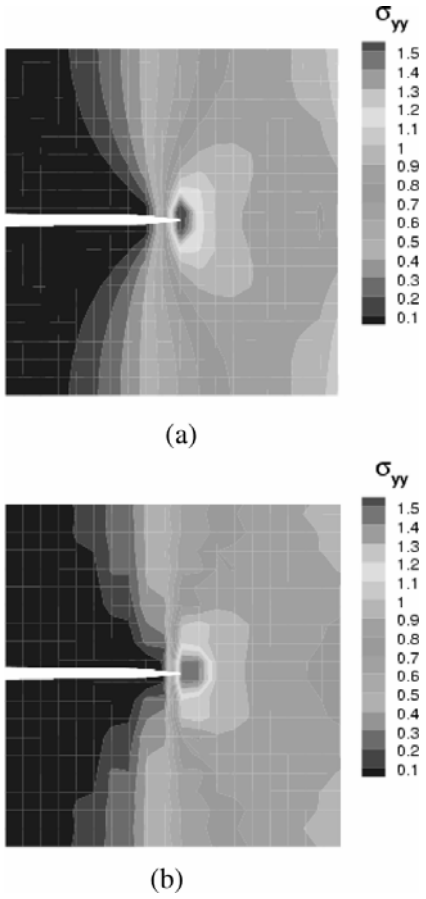

Acknowledgement

We are grateful for startup fund supports from the College of Engineering and the Centre for Computer-Aided Design (CCAD) at the University of Iowa.

References

Abraham, F., Broughton, J., Bernstein, N. and Kaxiras, E. (1998) 'Spanning the continuum to quantum length scales in a dynamic simulation of brittle fracture', *Europhysics Letters*, Vol. 44, pp.783–787.

Arroyo, M. and Belytschko, T. (2002) 'An atomistic-based finite deformation membrane for single layer crystalline films', *Journal of Mechanics and Physics in Solids*, Vol. 50, pp.1941–1977.

Beissel, S. and Belytschko, T. (1996) 'Nodal integration of the element-free Galerkin method', *Computer Methods in Applied Mechanics and Engineering*, Vol. 139, pp.49–74.

Belytschko, T., Liu, Y.Y. and Gu, L. (1994) 'Element-free Galerkin methods', *International Journal for Numerical Methods in Engineering*, Vol. 37, pp.229–256.

Belytschko, T., Krysl, P. and Krongauz, Y. (1997) 'A three-dimensional explicit element-free Galerkin method', *International Journal for Numerical Methods in Fluids*, Vol. 24, No. 12, pp.1253–1270.

Belytschko, T., Krongauz, Y., Dolbow, J. and Gerlach, C. (1998) 'On the completeness of meshfree particle methods', *International Journal for Numerical Methods in Engineering*, Vol. 43, pp.785–819.

Belytschko, T., Liu, W.K. and Moran, B. (2000) 'Nonlinear finite elements for continua and structures', New York: Wiley.

Belytschko, T. and Xiao, S. (2002) 'Stability analysis of particle methods with corrected derivatives', *Computers and Mathematics with Applications*, Vol. 43, pp.329–350.

Belytschko, T. and Xiao, S.P. (2003) 'Coupling methods for continuum model with molecular model', *International Journal for Multiscale Computational Engineering*, Vol. 1, No. 1, pp.115–126.

Broughton, J., Abraham, F., Bernstein, N. and Kaxiras, E. (1999) 'Concurrent coupling of length scales: methodology and application', *Physical Review B*, Vol. 60, pp.2391–2403.

Chen, J.S., Roque, C. and Pan, C.H. (1998) 'Analysis of metal forming process based on meshless method', *Journal of Materials Processing Technology*, Vol. 80, No. 1, pp.642–646.

Chen, S.Q., E, W. N. and Shu, C.W. (2005) 'The heterogeneous multiscale method based on the discontinuous galerkin method for hyperbolic and parabolic problems', *Multiscale Modelling and Simulation*, Vol. 3, No. 4, pp.871–894.

Dyka, C.T., Randles, P.W. and Ingel, R.P. (1997) 'Stress points for tension instability in SPH', *International Journal for Numerical Methods in Engineering*, Vol. 40, pp.2325–2341.

Fish, J. and Chen, W. (2004) 'Discrete-to-continuum bridging based on multigrid principles', *Computer Methods in Applied Mechanics and Engineering*, Vol. 193, pp.1693–1711.

Krysl, P. and Belytschko, T. (1999) 'The element free galerkin method for dynamic propagation of arbitrary 3-D cracks', *International Journal for Numerical Methods in Engineering*, Vol. 44, No. 6, pp.767–800.

Liu, W.K., Chen, Y., Jun, S., Chen, J.S., Belytschko, T., Pan, C., Uras, R.A. and Chang, C.T. (1996) 'Overview and applications of the reproducing kernel particle methods', *Archives of Computational Methods in Engineering: State of the Art Reviews*, Vol. 3, pp.3–80.

Liu, W.K., Hao, S., Belytschko, T., Li, S.F. and Chang, C.T. (1999) 'Multiple scale meshfree methods for damage fracture and localization', *Computational Materials Science*, Vol. 16, Nos. 1–4, pp.197–205.

Milstein, F. (1982) *Mechanics of Solids*, Oxford: Pergamon.

Park, H.S., Karpov, E.G., Liu, W.K. and Klein, P.A. (2005) 'The bridging scale for two-dimensional atomistic/continuum coupling', *Philosophical Magazine*, Vol. 85, No. 1, pp.79–113.

Rabczuk, T., Belytschko, T. and Xiao, S.P. (2004) 'Stable particle methods based on Lagrangian kernels', *Computer Methods in Applied Mechanics and Engineering*, Vol. 193, pp.1035–1063.

Randles, P. and Libersky, L. (1996) 'Smoothed particle hydrodynamics: some recent improvements and applications', *Computer Methods in Applied Mechanics and Engineering*, Vol. 139, pp.375–408.

Rodney, D. and Phillips, R. (1999) 'Structure and strength of dislocation junctions: an atomic level analysis', *Physical Review Letters*, Vol. 82, pp.1704–1707.

Shenoy, V., Shenoy, V. and Phillips, R. (1999) 'Finite temperature quasicontinuum methods', *Materials Research Society Symposium Proceeding*, Vol. 538, pp.465–471.

Tadmor, E.B., Ortiz, M. and Phillips, R. (1996) 'Quasicontinuum analysis of defects in solids', *Philosophy Magazine A*, Vol. 73, pp.1529–1563.

Xiao, S. and Belytschko, T. (2004) 'A bridging domain method for coupling continua with molecular dynamics', *Computer Methods in Applied Mechanics and Engineering*, Vol. 193, pp.1645–1669.